JOURNAL OF MATERIALS SCIENCE **34** (1999) 5811–5819

Reactions between $La_{1-x}Ca_xMnO_3$ and CaO-stabilized ZrO_2

Part II *Diffusion couples*

S. FAALAND, M.-A. EINARSRUD, K. WIIK, T. GRANDE
Department of Chemistry, Norwegian University of Science and Technology, 7491 Trondheim, Norway
E-mail: tor.grande@chembio.ntnu.no

R. HØIER
Department of Physics, Norwegian University of Science and Technology, 7491 Trondheim, Norway

The chemical stability of diffusion couples and coarse grain powder mixtures of calcium substituted lanthanum manganite and cubic calcia stabilized zirconia have been studied. The aim was to investigate the chemical stability of these materials as a model system for respectively the cathode and the electrolyte in solid oxide fuel cells. With increasing amount of Ca in lanthanum manganite, the major secondary phase was shifted from $La_2Zr_2O_7$ to $CaZrO_3$, and the thickness of the reaction layers of secondary phases was increasing with increasing heat treatment time. Precipitation of La_2O_3 had taken place in the perovskite containing low amounts of Ca (0 and 20 mol %). The transport mechanisms of the cations were strongly dependent on the interface geometry. $La_{0.7}Ca_{0.3}MnO_3$ was observed to give the most stable interface to zirconia both in air and in reducing atmosphere ($p_{O_2} \sim 10^{-6}$ atm). A-site deficiency of $LaMnO_3$ was also observed to increase the stability. However, we conclude that a thin film of an electrode material consisting of lanthanum manganite on a zirconia substrate is unstable, regardless of A-site deficiency, because the solubility limit of Mn in the zirconia is not reached. From the experimental data, a reaction mechanism has been proposed, based on observations of relative diffusion rates.

1. Introduction

The study of heterophase solid state interfaces becomes increasingly important due to numerous applications requiring long-time stability of such interfaces. In solid oxide fuel cells lanthanum manganite-based oxides, e.g. $La_{1-x}Ca_xMnO_3$ (LCM) and $La_{1-x}Sr_xMnO_3$ (LSM), are promising materials as cathodes because of their high electrical conductivity and relatively good compatibility with cubic stabilized zirconia which is the most common electrolyte. The reactivity of $La_{1-x}Ca_xMnO_3$ with yttria stabilized zirconia (YSZ) has been studied by several researchers [1–9]. In this work we have studied a model system for the electrode/electrolyte interface consisting of LCM and calcia stabilized zirconia (CSZ). The thermodynamic driving force for the formation of secondary phases is reduced in this system by replacing yttria in the zirconia with calcia. This substitution was performed in order to obtain a better understanding of the effect of different dopants on the stability of the electrode/electrolyte materials conventionally used in SOFC (LSM and YSZ) [1, 2]. We have in a first paper investigated the formation of secondary phases such as $La_2Zr_2O_7$ (LZ) and $CaZrO_3$ (CZ) during heat treatment of homogeneous sub micron powder mixtures of LCM and CSZ [10]. In this second paper, we report on an investigation on the chemical stability of solid state interfaces between LCM and CSZ in a model system consisting of diffusion couples of the two phases. The model resembles the geometry of SOFC, neglecting the contribution from the gradient in electrical potential and the partial pressure of oxygen during operation. The aim of the present investigation is twofold. Firstly, formation of secondary phases and elemental distributions in the heat treated diffusion couples are discussed as a function of partial pressure of oxygen. Secondly, the reaction mechanism is discussed based on observations as a function of time, interface geometry and A-site deficiency.

2. Experimental

Sub micron LCM powders containing 0, 20, 30, 40 and 60 mol % Ca on La site were prepared by means of the glycine/nitrate method as previously described [10]. In addition, a non-stoichiometric powder with

composition $La_{0.92}MnO_3$ was prepared by the same method. CSZ-powder with 17 mol % CaO (99.9%) was supplied from Seattle Specialty Ceramics, USA. The BET specific surface area was >3 m^2/g and the average grain-size was <1 μm.

Diffusion couples were prepared from sintered plates of CSZ and screen printed LCM films. Green plates of CSZ ($50 \times 10 \times 4$ mm^3) were uniaxially pressed (38–45 MPa) using poly vinyl alcohol (1.5 wt %) and poly ethylene glycol (1.5 wt %) as respectively binder and plasticizer. The green density obtained was 40–45% of theoretical. The plates were sintered in air at 1650 °C for 1 h obtaining a density >90% of theoretical. Screen printing pastes were prepared by adding wax (Bronze-binder, TBK Siebdruck Hilfsmittel, Marabu) to the calcined LCM powder in a mass ratio 1 : 1.25. The LCM films of 1×1 cm^2 and 25 μm thickness were screen printed on the sintered CSZ plates and fired at 1350 °C with dwelling times from 15 min to 120 h in air or in reducing atmosphere ($p_{O_2} \sim 10^{-6}$ atm). The average heating- and cooling rate of the samples fired for 120 h was 200 °C/h indicating that the samples have spent 3 h above 1000 °C during heating and cooling from 1350 °C. The samples fired for 1 h were subjected to a heating rate of approximately 4200 °C/h and a cooling rate of approximately 2700 °C/h giving an excess time above 1000 °C of 13 min. The samples fired for 15 min or less, were placed directly into the furnace at 1350 °C and removed at the same temperature giving nearly no excess time above 1000 °C.

To study the reaction mechanism of the interface between LCM and CSZ more in detail a 1 : 1 mass ratio of $La_{1-x}Ca_xMnO_3$ ($x = 0.2$ and 0.6) and CSZ was prepared by dry ball-milling of large (50–150 μm diameter) porous agglomerates of both phases. These mixtures are labeled 'large grain samples' in the following. The samples were fired in air for 120 h at 1350 °C with a heating- and cooling rate of 200 °C/h.

The cross sections of the diffusion couples were investigated by scanning electron microscopy (SEM) (Zeiss DSM 940) and transmission electron microscopy (TEM)(Philips CM30, 300 kV) both equipped with energy dispersive spectroscopy (EDS) systems for micro-analysis. Cross sections of the diffusion couples and 'large grain samples' were mounted in an electrically conductive resin (Condufast, Struers), ground and polished for SEM investigation. Diffusion couples were prepared for TEM investigation by dividing, polishing and Ar-ion beam thinning. X-ray maps (128×128) were recorded of the elements Ca, La, Mn and Zr using an acquisition time of 0.5 s per point.

The diffusion couples were subjected to X-ray diffraction (XRD), Philips PW 1050/25 and Siemens D5005, after heat treatment. Formation of secondary phases was identified using Cu_{K_α} radiation and scan rates of 0.01°/s to 0.05°/s.

3. Results and discussion

3.1. Formation of secondary phases and elemental distrubutions

Chemical reactions at the interface between LCM and CSZ are expected based on the equilibrium phase compositions observed in heat treated powder mixtures of the corresponding primary phases [10]. The formation of secondary phases in all the samples studied is summarized in Table I. Backscattered electron (BSE) images of $La_{0.7}Ca_{0.3}MnO_3$/CSZ and $La_{0.4}Ca_{0.6}MnO_3$/CSZ diffusion couples fired in air are shown in Fig. 1. In the $La_{0.7}Ca_{0.3}MnO_3$/CSZ diffusion couple no secondary phases were detected by SEM after 1 h at 1350 °C, indicating that this composition is the most stable composition in air. In the $La_{0.4}Ca_{0.6}MnO_3$/CSZ diffusion couple, no secondary phases were detected by SEM after 15 min at 1350 °C. However, after 1 h at 1350 °C a ~2.5 μm thick layer of CZ was formed. This sample was used for determining the transport rate coefficient for the formation of the CZ-phase. If the rate of CZ formation is limited by solid state diffusion

TABLE I Survey of secondary phases formed at $La_{1-x}Ca_xMnO_3$/CSZ interfaces identified by SEM/EDS and XRD

	Air				Reducing atmosphere ($p_{O_2} \sim 10^{-6}$ atm)			
	1 h		120 h		1 h		120 h	
Nominal x in $La_{1-x}Ca_xMnO_3$	Phases	Thickness (μm)	Phases	Thickness (μm)	Phases	Thickness (μm)	Phases	Thickness (μm)
0.0	LO	1	LO	2	LZ	4	LZ	*[a]
			LZ	2	CZ	traces	CZ	traces
0.2	LO	traces	LO	2				
			LZ	2	#[b]		#[b]	
			CZ	2				
0.3	—[c]		LZ	Discrete	LZ	traces	LZ	2
			CZ	fragments	CZ	3	CZ	3
0.4	—[c]		LZ	1	#[b]		#[b]	
			CZ	1				
0.6	CZ	2.5	LZ	1	CZ	*[a]	CZ	*[a]
			CZ	7			LZ	traces

(La, Ca)MnO_3 = LCM; ZrO_2(CaO) = CSZ; $La_2Zr_2O_7$ = LZ; $CaZrO_3$ = CZ; La_2O_3 = LO.
[a]no LCM left.
[b]not analysed.
[c]no secondary phases observed.

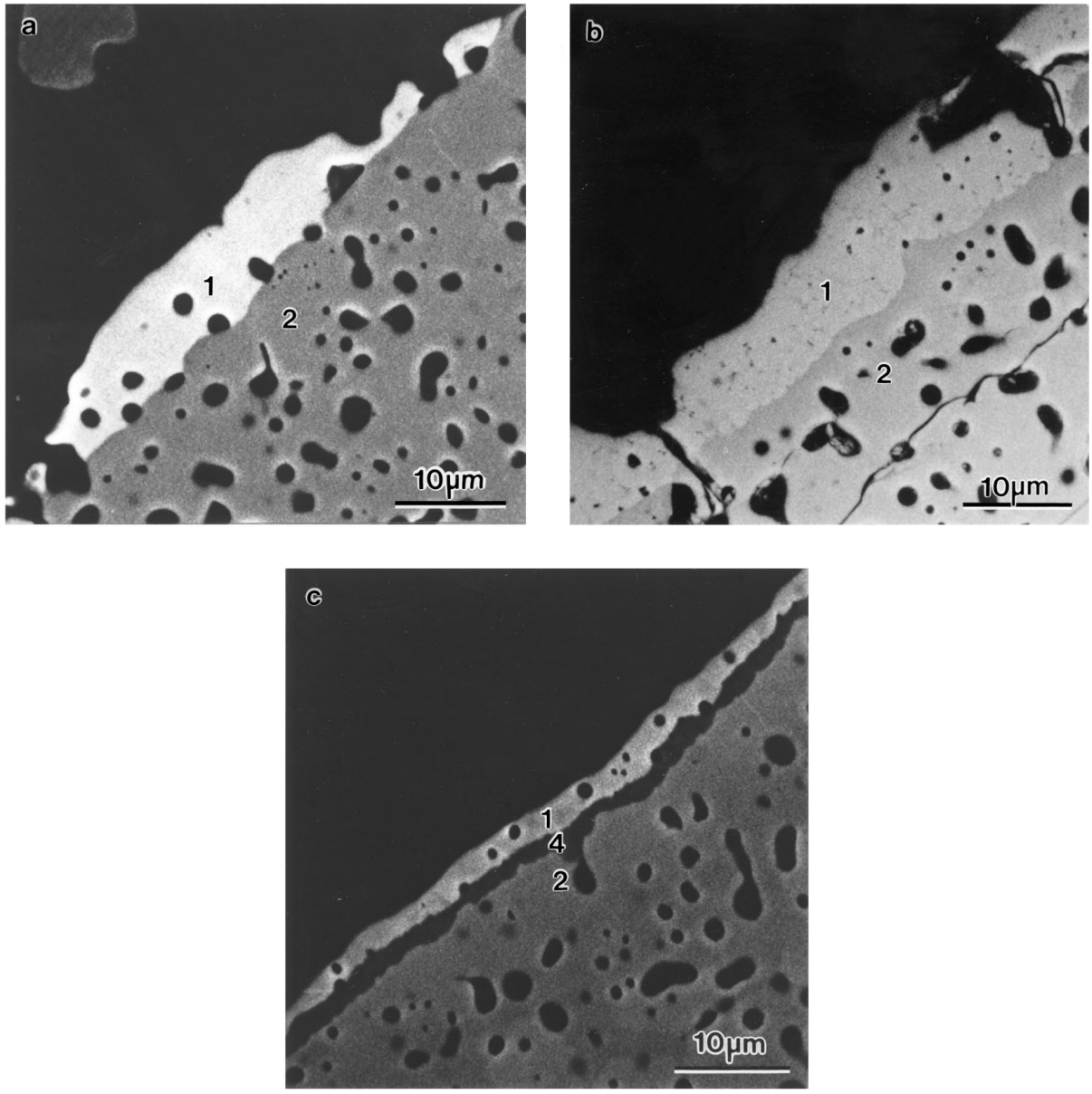

Figure 1 BSE images of (a) $La_{0.7}Ca_{0.3}MnO_3$/CSZ fired for 1 h at 1350 °C, and $La_{0.4}Ca_{0.6}MnO_3$/CSZ fired for (b) 15 min and (c) 1 h at 1350 °C. Note that the closed porosity in the zirconia layer is present prior to the exposure to the manganite. 1 = LCM, 2 = CSZ, 4 = CZ.

through the CZ-layer, the thickness, x, of the newly formed phase must obey the parabolic rate law

$$x^2 = 2k_p t \tag{1}$$

where t is time and k_p is a transport coefficient related to solid state diffusion [11]. The transport rate coefficient thus calculated is of the order 10^{-15} m^2/s. Tagawa *et al.* [6] found that the rate of CZ formation in a $La_{0.6}Ca_{0.4}CoO_3$/YSZ diffusion couple corresponds to a transport rate coefficient of $k_p \sim 10^{-10}$ m^2/s at 1200 °C. Due to the higher temperature in the present work, the formation of CZ in the LCM/CSZ system is significantly slower, indicating a higher stability of this system. Further investigations on the $La_{0.4}Ca_{0.6}MnO_3$/CSZ diffusion couple were performed to gain knowledge about nucleation of the CZ-phase.

After heat treatment at 1350 °C for 120 h, all five diffusion couples show one or several reaction layers at the LCM/CSZ interface (Table I). BSE images of selected diffusion couples fired in air at 1350 °C for 120 h are given in Fig. 2. The phase composition and thickness of the reaction layers were dependent on the Ca content in LCM. In the $LaMnO_3$/CSZ diffusion couple (Fig. 2a) there is a reaction layer of LZ in agreement with the secondary phase observed in heat treated powder mixtures of the corresponding primary phases [9, 10, 12]. With increasing amount of Ca in LCM, the major secondary phase is shifted from LZ to CZ. The reaction layers were most pronounced for the $La_{0.4}Ca_{0.6}MnO_3$/CSZ diffusion couple as shown in Fig. 2d, where a ~1 μm thick layer of LZ and a ~7 μm thick layer of CZ were formed at the phase boundary after firing for 120 h at 1350 °C. The thickness of the CZ layer was significantly thinner (~1 μm) in the diffusion couple $La_{0.6}Ca_{0.4}MnO_3$/CSZ, while only discrete fragments of a thin (~1 μm) CZ layer could be observed by SEM in the $La_{0.7}Ca_{0.3}MnO_3$/CSZ diffusion couple (Fig. 2c). Note also that exsolution of La_2O_3 (LO) has

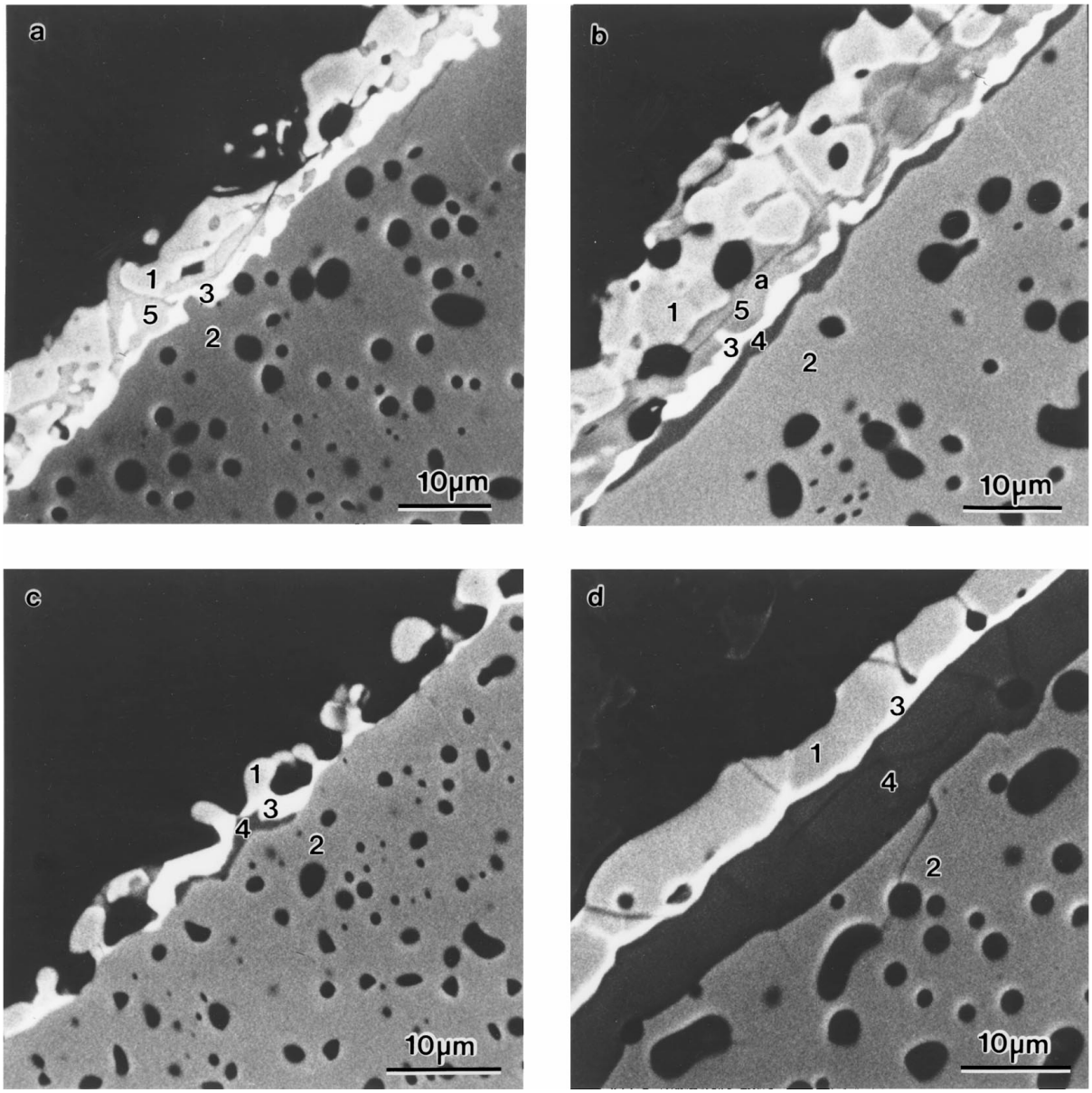

Figure 2 BSE images of (a) $LaMnO_3$/CSZ, (b) $La_{0.8}Ca_{0.2}MnO_3$/CSZ, (c) $La_{0.7}Ca_{0.3}MnO_3$/CSZ and (d) $La_{0.4}Ca_{0.6}MnO_3$/CSZ diffusion couples fired for 120 h at 1350 °C in air. Note that the closed porosity in the zirconia layer is present prior to the exposure to the manganite. 1 = LCM, 2 = CSZ, 3 = LZ, 4 = CZ, 5 = LO.

taken place in the LCM layers containing a low amount of Ca.

According to Gibbs phase rule, $p + f = c + 2$, where p is the number of phases, f is the number of degrees of freedom and c is the number of components (Ca, La, Mn, O, Zr $\Rightarrow c = 5$), at a given temperature ($T = 1350\,^{\circ}C$) and pressure ($p_{O_2} \sim 10^{-6}$ atm) the maximum number of phases at equilibrium is 5 (4 solid phases + O_2(g)). Thus, due to the presence of five solid phases (LCM, LO, LZ, CZ, CSZ) in $La_{0.8}Ca_{0.2}MnO_3$/CSZ, this diffusion couple is not in chemical equilibrium after 120 h at 1350 °C. Compared to the equilibrium phase compositions observed in heat treated powder mixtures of the corresponding primary phases [10], it can be concluded that the reaction kinetics is much slower in the diffusion couples. The phases present are dependent on the Ca content in LCM (Fig. 2), however, the sequence of the phases, LCM-LO-LZ-CZ-CSZ, is always the same irrespective of which phases are present. Based on the sequence of the phases and the presence of phases after short (1 h) and long (120 h) time at 1350 °C (Fig. 2 and Table I), it can be concluded that for samples with a low amount of Ca in the perovskite ($x = 0$, 0.2) LO is formed before LZ and CZ ($x = 0.2$). A high amount of Ca ($x = 0.4$, 0.6) causes formation of CZ prior to LZ. It is known that all the cations in the present system possess considerable solid solubility in the cubic form of ZrO_2 [13–15]. The solubility of MnO in ZrO_2 is approximately 20 wt % under reducing conditions [15]. Mn was found to be homogeneously distributed in the CSZ-phase, as shown in Fig. 3 for the $LaMnO_3$/CSZ diffusion couple fired for 120 h at 1350 °C.

Formation of LO was observed in the $LaMnO_3$/CSZ and $La_{0.8}Ca_{0.2}MnO_3$/CSZ diffusion couples after 1 and 120 h at 1350 °C (Fig. 2a and b). The presence of LO at the interface was confirmed by element analysis (X-ray mapping) reported in Fig. 3a and X-ray diffraction.

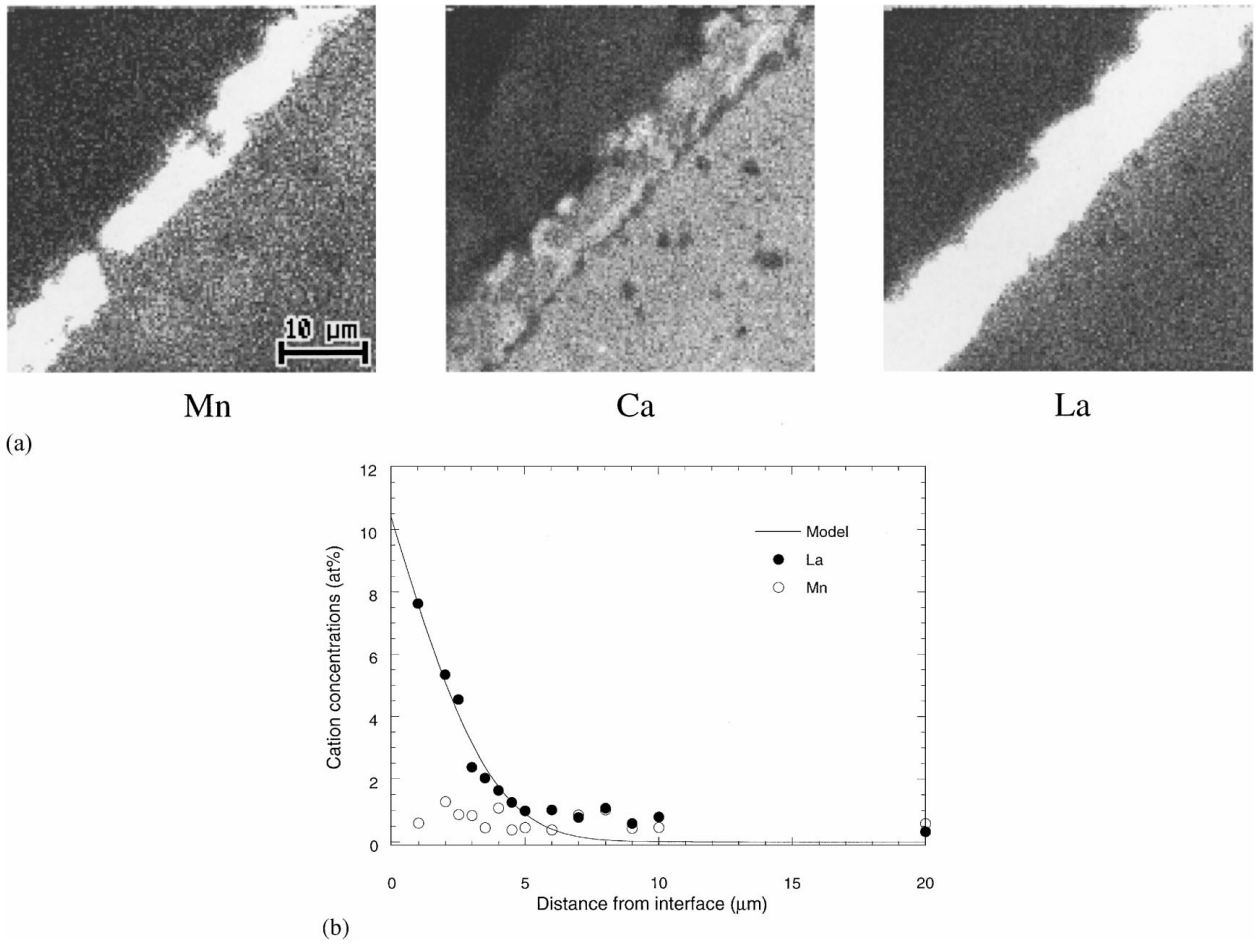

Figure 3 (a) X-ray maps of the diffusion couple $LaMnO_3$/CSZ fired for 120 h at 1350 °C. The lighter areas in the X-ray maps indicate areas of high element-concentration. (b) Diffusion profile of La and Mn into the CSZ-phase. The standard deviations in the measurements are ∼1 at %. Fit of Equation 2 to the La-data is given by the model.

From the element analysis, it is evident that the amount of Ca in the LO-phase is high. According to the CaO–La_2O_3 phase diagram [16] the solubility of CaO in La_2O_3 at 1350 °C is ∼8 mol %. Substitution of La^{3+} ($r_{La^{3+}} = 1.06$ Å, CN = 6) with Ca^{2+} ($r_{Ca^{2+}} = 1.00$ Å, CN = 6) [17] causes a contraction of the unit cell. The lattice parameters of the Ca-rich monoclinic LO-phase were calculated to be $a = 14.539(5)$Å, $b = 3.677(4)$Å, $c = 9.178(6)$Å and $\beta = 99.86(4)^\circ$, consistent with a unit cell volume of 483.5(3)Å^3. The unit cell volume of pure La_2O_3 is 496.08 Å^3 [18].

Formation of manganese oxide was not observed in any of the heat treated diffusion couples. This phenomenon is explained by the diffusion of Mn into CSZ (Fig. 3a) and the dissolved Mn in the secondary phases LZ and CZ. Kleveland *et al.* [2], on the other hand, observed formation of manganese oxide in $La_{0.4}Sr_{0.6}MnO_3$/YSZ diffusion couples after 1 h heat treatment at 1350 °C. In the present LCM/CSZ system the diffusion depth of Mn into CSZ is much larger than the diffusion depth of La (Fig. 3b). In fact, we observe an almost constant Mn-concentration throughout the CSZ-phase. Taimatsu *et al.* [9], on the other hand, observed gradually decreasing concentrations of Mn and La in a LM/YSZ diffusion couple. Clausen *et al.* [19] also observed Mn diffusion into YSZ in a $La_{0.85}Sr_{0.15}MnO_3$/YSZ diffusion couple. Mn-diffusion into YSZ was observed to cause Mn depletion of LSM, and in the case of stoichiometric LSM, LO was formed at the interface. In the LCM/CSZ system LO is formed when the Ca content in LCM is <30 mol %.

The effect of the partial pressure of oxygen was studied by firing $La_{1-x}Ca_xMnO_3$/CSZ, $x = 0$, 0.3 and 0.6, diffusion couples in reducing atmosphere ($p_{O_2} \sim 10^{-6}$ atm) for 1 and 120 h at 1350 °C. By comparing the micro graphs in Fig. 2 and Fig. 4 it is evident that the atmosphere strongly influences the phase distribution. As for powder mixtures of LCM and CSZ studied by Faaland *et al.* [10], diffusion couples are observed to be more reactive in reducing atmosphere than in air. In the $LaMnO_3$/CSZ sample all of the lanthanum manganite is transformed into LZ. Similarly, in the $La_{0.4}Ca_{0.6}MnO_3$/CSZ sample all the perovskite has reacted to CZ. Thus, after 120 h at 1350 °C only the $La_{0.7}Ca_{0.3}MnO_3$/CSZ diffusion couple has some perovskite left, indicating that this composition is the most stable also in reducing atmosphere.

3.2. Reaction mechanism

Further investigations on the $La_{0.4}Ca_{0.6}MnO_3$/CSZ diffusion couple fired in air for 15 min at 1350 °C were done by TEM to gain knowledge about nucleation of the CZ-phase. A TEM-image of the $La_{0.4}Ca_{0.6}MnO_3$/CSZ

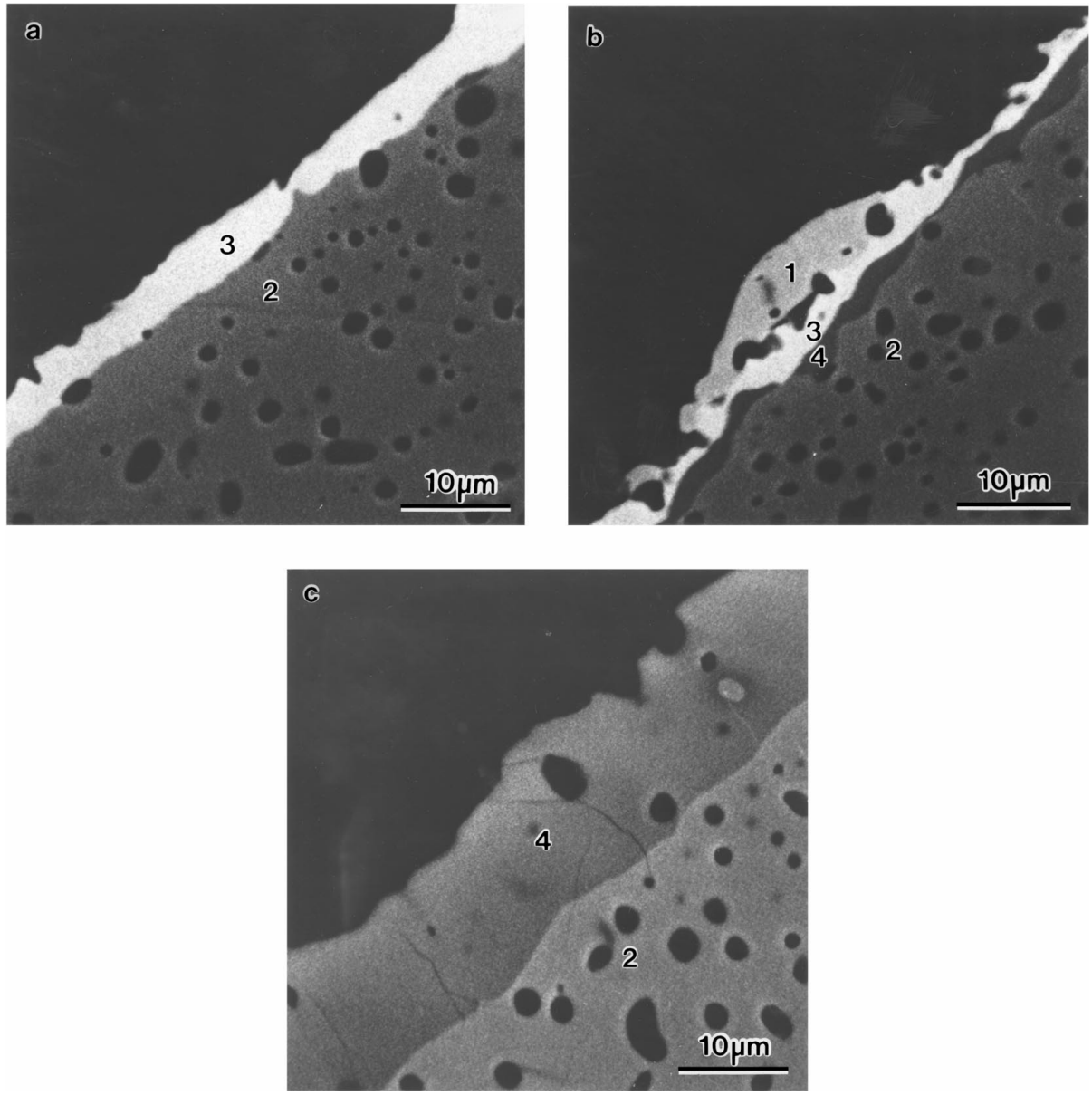

Figure 4 BSE images of (a) $LaMnO_3$/CSZ, (b) $La_{0.7}Ca_{0.3}MnO_3$/CSZ and (c) $La_{0.4}Ca_{0.6}MnO_3$/CSZ diffusion couples fired for 120 h at 1350 °C in reducing atmosphere ($p_{O_2} \sim 10^{-6}$ atm). Note that the closed porosity in the zirconia layer is present prior to the exposure to the manganite. 1 = LCM, 2 = CSZ, 3 = LZ, 4 = CZ.

interface is shown in Fig. 5. Formation of a thin (0.1–0.2 μm) layer of a secondary phase is evident. The secondary phase was characterized by selected area electron diffraction (SAED) (Fig. 5 inset) and EDS, both methods indicating the ordered phase $Ca_6Zr_{19}O_{44}$ where the coordination of zirconium is 8-fold as in the fluorite structure of ZrO_2. This observation may suggest that the $Ca_6Zr_{19}O_{44}$-phase appears as a precursor to the formation of $CaZrO_3$. Yin and Argent [20] studied the partial phase diagram of the system ZrO_2-CaO and found the ordered phase $Ca_6Zr_{19}O_{44}$ to be present at 1300 °C but not at 1370 °C. This temperature interval was close to Stubican's observation [21, 22], hence their measured value 1355 ± 15 °C was accepted as the decomposition temperature. $Ca_6Zr_{19}O_{44}$ is the only stable phase between ZrO_2 and $CaZrO_3$ at 1350 °C according to the ZrO_2-CaO phase diagram by Yin and Argent [20]. Thus, we assume that a chemical reaction transforming $Ca_6Zr_{19}O_{44}$ to $CaZrO_3$ takes place during the first hour at 1350 °C. This assumption was further confirmed by EDS-micro-analyses of the secondary phase in different areas of the interface which gave a Zr to Ca ratio varying between 1.7 and 3.1.

BSE images of $La_{0.4}Ca_{0.6}MnO_3$/CSZ and $La_{0.8}Ca_{0.2}MnO_3$/CSZ 'large grain samples' fired for 120 h at 1350 °C are shown in Fig. 6. It is evident that only one secondary phase is formed in each sample: CZ in $La_{0.4}Ca_{0.6}MnO_3$/CSZ and LZ in $La_{0.8}Ca_{0.2}MnO_3$/CSZ. It is also evident that both secondary phases grow into the CSZ phase. The major mass transport mechanism is obviously surface diffusion in both cases due to the preferred growth of the secondary phases along the CSZ-surface (Fig. 6). In the corresponding diffusion couples several reaction layers are formed (Fig. 2b, d), indicating that the reaction mechanism is dependent on the interface geometry. The 'large grain samples' have high porosity. Thus, the free surface area is high, enhancing surface diffusion of Ca^{2+}, La^{3+} and Zr^{4+} which is much faster than bulk diffusion of these elements through a reaction layer. Mitterdorfer *et al.* [12] found

Figure 5 TEM image of $La_{0.4}Ca_{0.6}MnO_3$/CSZ diffusion couple fired for 15 min at 1350 °C. Formation of a secondary phase (marked by *X*), $Ca_6Zr_{19}O_{44}$, at the interface is shown. (inset) [0 1 0] zone-axis pattern of $Ca_6Zr_{19}O_{44}$. The a*- and c*-directions of the hexagonal cell are indicated. The crystal structure indexing is based on the hexagonal cell with $a_H = 27.366$ Å and $c_H = 11.713$ Å given by Yin and Argent [20].

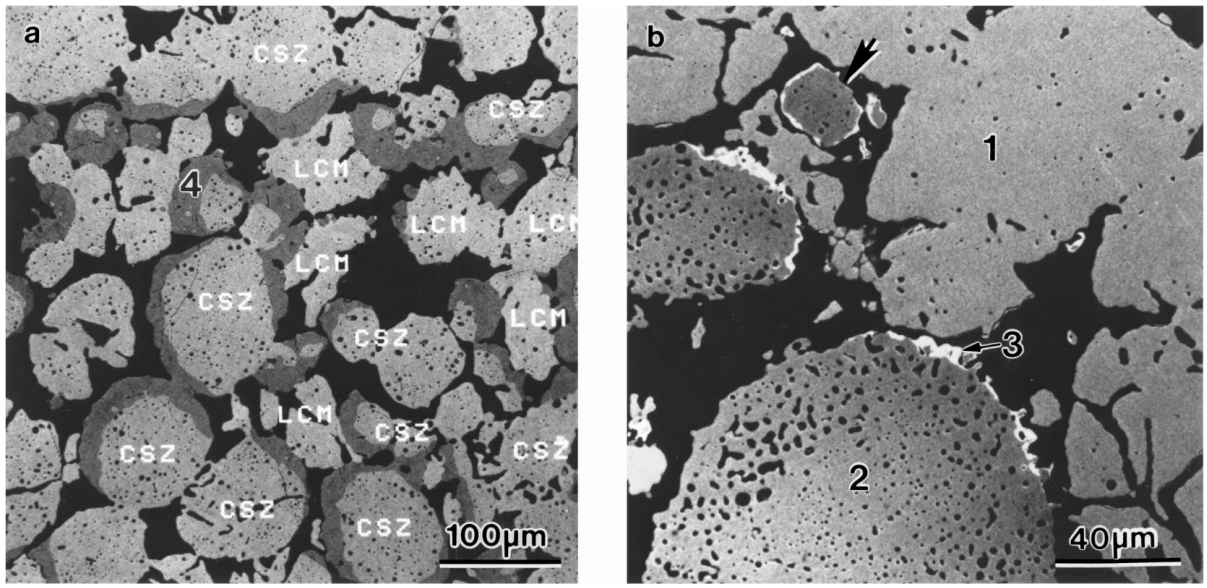

Figure 6 BSE images of (a) $La_{0.4}Ca_{0.6}MnO_3$/CSZ and (b) $La_{0.8}Ca_{0.2}MnO_3$/CSZ 'large grain samples' fired for 120 h at 1350 °C. Note the reduced LZ-formation when a small CSZ-agglomerate (marked by an arrow) is surrounded by significantly larger LCM-agglomerates. 1 = LCM, 2 = CSZ, 3 = LZ, 4 = CZ.

that the growth of LZ in an LSM/YSZ diffusion couple was limited at the early stage of sintering by surface diffusion of La^{3+} and Zr^{4+}.

Concerning the diffusion of Mn, there is a significant difference between the LCM/CSZ diffusion couples in the present work and the electrode/electrolyte materials conventionally used in SOFC, i.e. LSM and YSZ. In LSM/YSZ diffusion couples Mn has been observed to diffuse into YSZ along grain boundaries [2, 23, 24] ($D_{Mn} = 10^{-13}$ m^2/s [23]), while in the LCM/CSZ

diffusion couples we observe Mn homogeneously distributed in the CSZ-phase, indicating volume diffusion of Mn into CSZ. The Mn concentration is ∼1 mol % throughout the CSZ-phase as can be seen in Fig. 3b. The diffusion coefficient of Mn in CSZ is thus relatively high. The diffusion coefficient of La in CSZ can be estimated from the data shown in Fig. 3b. Due to the large grains of CSZ (>5 μm), it seems reasonable to assume that only unidirectional diffusion of La into CSZ occurs. The boundary, $y = 0$, is maintained at constant concentration, c_0, i.e. the solubility limit of La_2O_3 in the CSZ. If the diffusion constant, D_{La}, is constant in the diffusion zone and no expansion of this zone occurs during diffusion, then the solution to the diffusion equation is given as

$$c(y, t) = c_0 \quad erfc\left(\frac{y}{2\sqrt{Dt}}\right) \tag{2}$$

where $c(y, t)$ is the concentration at distance y and annealing time t [25]. Thus, Equation 2 enables the estimation of an approximate value of the diffusion coefficient. Fit of Equation 2 to the La-data shown in Fig. 3b gives $c_0 = 10.4$ at % and $D_{La} = 10^{-17}$ m^2/s. According to Taimatsu *et al.* [9] the diffusion coefficient of La in single-crystal ZrO_2 containing 8 mol % Y_2O_3 at 1400 °C is $D_{La} = 2 \times 10^{-18}$ m^2/s. As can be seen from Fig. 3b the fit of Equation 2 to the La-data is rather accurate at distances less than 5 μm. Hence, due to the large grains of CSZ and no segregation of La at grain boundaries, the main mass transport mechanism close to the interface is volume diffusion. However, for $y > 5$ μm the estimated concentration from the model is too low, indicating a higher diffusion coefficient due to the contribution of grain boundary diffusion.

Clausen *et al.* [19] observed that in the case of a low YSZ/LSM ratio in a powder mixture, Mn was dissolved in the YSZ and excess Mn was still available in the LSM, preventing formation of LO at the interface and thus LZ formation. In the 'large grain samples' pyrochlore formation is not prevented but considerably reduced when a small CSZ-agglomerate is surrounded by significantly larger LCM-agglomerates as can be seen in Fig. 6b. Hence, we assume that a thin film of an electrode material consisting of lanthanum manganite on a zirconia substrate is unstable, regardless of A-site deficiency, because the solubility limit of Mn in the zirconia is not reached. To confirm this assumption the $La_{0.92}MnO_3$/CSZ diffusion couple was studied. The BSE-image (Fig. 7) reveals a 2–3 μm thick layer of LZ comparable to the pyrochlore layer formed in the stoichiometric $LaMnO_3$/CSZ diffusion couple. However, in the La-deficient $La_{0.92}MnO_3$/CSZ sample, no LO is observed after 120 h at 1350 °C, indicating that all excess LO from the Mn-deficient LM has reacted with CSZ to form a homogeneous layer of LZ. Note also the large pores at the LM/LZ interface due to the evolution of oxygen during formation of LZ [10].

The results obtained in the present work can be explained by the following reaction mechanisms:

(1) $LaMnO_3$/CSZ: i) Mn ions are transported by volume diffusion into the CSZ phase in larger quantity than La ions. ii) The lanthanum manganite (LM) phase near the CSZ gradually becomes deficient in Mn and enriched in La. iii) Excess LO from the Mn-deficient LM is chemically active and reacts with CSZ to form a homogeneous layer of LZ. The process is facilitated in the 'large grain samples' which allow both surface diffusion of the participating elements and oxygen exchange with the surrounding atmosphere. In the diffusion couples, further growth is limited by volume/grain boundary diffusion of La^{3+} through LZ, which is much slower than surface diffusion. Thus, precipitation of LO is observed in the diffusion couples and not in the 'large grain samples'. The LZ-layer, however, grows at the LZ/CSZ interface in both cases. Thus, the diffusion of Zr^{4+} through LZ is less significant. In the La-deficient $La_{0.92}MnO_3$/CSZ sample, no LO is observed after 120 h at 1350 °C, indicating that all excess LO from the Mn-deficient LM has reacted with CSZ to form LZ.

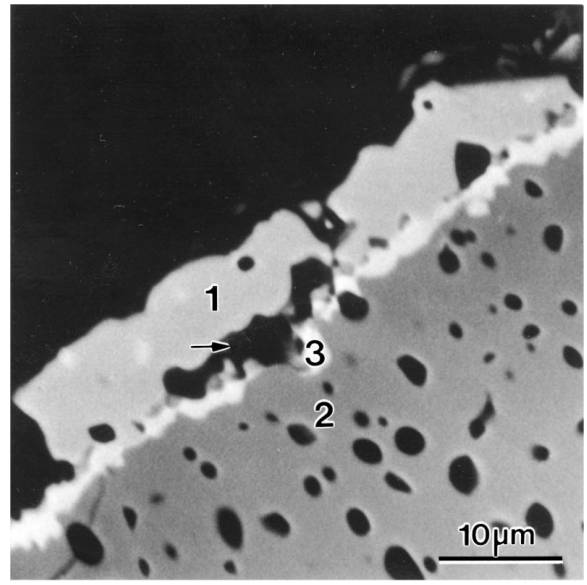

Figure 7 BSE image of the A-site deficient $La_{0.92}MnO_3$/CSZ diffusion couple fired for 120 h at 1350 °C in air. The large pores marked by an arrow are due to the evolution of oxygen during formation of LZ [10]. 1=LCM, 2=CSZ, 3=LZ.

(2) $La_{0.4}Ca_{0.6}MnO_3$/CSZ: The substitution of Ca for La in $LaMnO_3$ suppresses the diffusion of Mn ions into CSZ probably due to the increase in the average oxidation state of the Mn ion with the substitution of Ca^{2+} for La^{3+}. However, the reaction mechanism includes: i) Unidirectional diffusion of Ca and Mn into the CSZ-phase. ii) Nucleation of the CZ precursor, $Ca_6Zr_{19}O_{44}$, at the interface. iii) Chemical reaction transforming $Ca_6Zr_{19}O_{44}$ to CZ during the first hour at 1350 °C. As for the formation of LZ, the formation of CZ is facilitated in the 'large grain samples' which allows surface diffusion of Ca ions and oxygen exchange with the surrounding atmosphere. In the $La_{0.4}Ca_{0.6}MnO_3$/CSZ diffusion couple fired for 120 h at 1350 °C also traces of LZ were observed due to the diffusion of Zr^{4+} through the CZ-layer, indicating that CZ is formed preliminary to LZ.

Both reaction mechanisms are accelerated in reducing atmosphere compared to air, due to the reductive

nature of the reaction between LCM and CSZ [10]. The reaction mechanism for the $La_{1-x}Ca_xMnO_3$/CSZ diffusion couples with $x = 0.2$, 0.3 and 0.4 is a combination of mechanisms (1) and (2).

Formation of secondary phases in lanthanum manganite (LXM $X = Ca, Sr$)/yttria stabilized zirconia (YSZ) systems has been studied by several researchers [1–9]. Nucleation is found to occur at the LXM/YSZ interface, but there is a disagreement on whether grains of the secondary phases grow into the YSZ-phase, the LXM-phase or both. In the present LCM/CSZ system we observed nucleation of LZ/CZ at the LCM/CSZ interface, and further growth mainly into the CSZ-phase. A reaction mechanism has been proposed by Taimatsu *et al.* [9] for the formation of LZ at the $La_{1-x}Ca_xMnO_3$/YSZ ($x = 0$, 0.1, 0.2) boundary. Mn ions are assumed to diffuse faster than La-ions into YSZ, and subsequently the remaining LO reacts with ZrO_2 to form LZ. La and Mn ions diffuse unidirectionally through the LZ layer, and this layer grows at the LZ/YSZ interface. Thus, the reaction mechanisms presented here for the LCM/CSZ system have much in common with the reaction mechanism proposed by Taimatsu *et al.* [9].

4. Conclusions

The present investigation has shown that LCM and CSZ are not coexistent phases. The rate of formation of secondary phases, however, is strongly dependent on the Ca-content of the perovskite and the heterophase interface geometry. The most chemically stable interface was observed when the lanthanum manganite contained 30 mol % Ca on La-site both in air and in reducing atmosphere ($p_{O_2} \sim 10^{-6}$ atm). However, the stability was decreasing with decreasing partial pressure of oxygen. 8 mol % A-site deficiency of LM only gave an insignificant stabilizing effect. Hence, we conclude that a thin film of an electrode material consisting of lanthanum manganite on a zirconia substrate is unstable, regardless of A-site deficiency, because the solubility limit of Mn in the zirconia is not reached. From the experimental data, a reaction mechanism has been proposed, based on observations of relative diffusion rates.

Acknowledgements

The authors wish to thank the Norwegian scientific foundation VISTA for financial support.

References

1. K. WIIK, C. R. SCHMIDT, S. FAALAND, S. SHAMSILI, M.-A. EINARSRUD and T. GRANDE, *J. Amer. Ceram. Soc.* **82**(3) (1999) 721.
2. K. KLEVELAND, M.-A. EINARSRUD, C. R. SCHMIDT, S. SHAMSILI, S. FAALAND, K. WIIK and T. GRANDE, *ibid.* **82**(3) (1999) 729.
3. H. KANEKO, H. TAIMATSU, K. WADA and E. IWAMOTO, Proceedings of the Second International Symposium on Solid Oxide Fuel Cells, Athens, 1991, edited by F. Gross, P. Zegers, S. C. Singhal and O. Yamamoto, p. 673.
4. J. MIZUSAKI, H. TAGAWA, K. TSUNEYOSHI and A. SAWATA, *J. Electrochem. Soc.* **138**(7) (1991) 1867.
5. J. MIZUSAKI, H. TAGAWA, K. TSUNEYOSHI, A. SAWARA, M. KATOU and K. HIRANO, *Denki Kagaku* **58**(6) (1990) 520.
6. H. TAGAWA, J. MIZUSAKI, M. KATOU, K. HIRANO, A. SAWATA and K. TSUNEYOSHI, Proceedings of the Second International Symposium on Solid Oxide Fuel Cells, Athens, 1991, edited by F. Gross, P. Zegers, S. C. Singhal and O. Yamamoto, p. 681.
7. Y. TAKEDA, Y. SAKAI, T. ICHIKAWA, N. IMANISHI and O. YAMAMOTO, *Solid State Ionics* **72** (1994) 257.
8. K. TSUNEYOSHI, K. MORI, A. SAWATA, J. MIZUSAKI and H. TAGAWA, *ibid.* **35** (1989) 263.
9. H. TAIMATSU, K. WADA, H. KANEKO and H. YAMAMURA, *J. Amer. Ceram. Soc.* **75**(2) (1992) 401.
10. S. FAALAND, M.-A. EINARSRUD, K. WIIK and T. GRANDE, *J. Mater. Sci.* **34** (1999) 957.
11. H. SCHMALZRIED, in "Chemical Kinetics of Solids" (VCH, Weinheim, 1995) p. 153.
12. A. MITTERDORFER, M. CANTONI and L. J. GAUCKLER, Proceedings of the Second European Solid Oxide Fuel Cell Forum, Oslo, May 1996, edited by B. Thorstensen, p. 373.
13. A. ROUANET, *Rev. Int. Hautes Temp. Refract.* **8** (1971) 161.
14. T. NOGUCHI and O. YONEMOCHI, *J. Amer. Ceram. Soc.* **52** (1969) 178.
15. R. L. SHULTZ and A. MUAN, *ibid.* **54** (1971) 504.
16. L. M. LOPATO, L. I. LUGIN, G. I. GERASIMYUK and A. V. SHEVCHENKO, *Ukr. Khim. Zh.* **38**(2) (1972) 143.
17. R. D. SHANNON and C. T. PREWITT, *Acta Cryst.* **B25** (1968) 925.
18. WILLER and DAIRE, *Bull. Soc. Fr. Mineral. Cristallogr.* **92** (1969) 33.
19. C. CLAUSEN, C. BAGGER, J. B. BILDE-SØRENSEN and A. HORSEWELL, *Solid State Ionics* **70/71** (1994) 59.
20. Y. YIN and B. B. ARGENT, *J. Phase Equilibria* **14**(4) (1993) 439.
21. J. R. HELLMANN and V. S. STUBICAN, *J. Amer. Ceram. Soc.* **66** (1983) 260.
22. V. S. STUBICAN, G. S. CORMAN, J. R. HELLMANN and G. SENFT, in 'Advances in Ceramics' 12 Science and Technology of Zirconia II, edited by N. Claussen, M. Ruhle and A. H. Heuer (Am. Ceram. Soc., 1984) p. 96.
23. S. K. LAU and S. C. SINGHAL, in 'Corrosion 85: The International Corrosion Forum Devoted to the Protection and Performance of Materials, Boston, March 1985' (NACE, Houston, 1985) p. 79.
24. J. D. CARTER, C. C. APPEL and M. MOGENSEN, *J. Solid State Chem.* **122** (1996) 407.
25. H. S. CARSLAW and J. C. JAEGER, in "Conduction of Heat in Solid," 2nd ed. (Oxford University Press, Oxford, 1959) p. 60.

Received 22 September1998
and accepted 3 June 1999